



**HAL**  
open science

## Carbonation of Vegetable Oils: Influence of Mass Transfer on Reaction Kinetics

Jun Zheng, Fabrice Burel, Tapio Salmi, Bechara Taouk, Sébastien Leveneur

► **To cite this version:**

Jun Zheng, Fabrice Burel, Tapio Salmi, Bechara Taouk, Sébastien Leveneur. Carbonation of Vegetable Oils: Influence of Mass Transfer on Reaction Kinetics. *Industrial and engineering chemistry research*, 2015, 54 (43), pp.10935-10944. 10.1021/acs.iecr.5b02006 . hal-02138621

**HAL Id: hal-02138621**

**<https://normandie-univ.hal.science/hal-02138621v1>**

Submitted on 17 Jan 2022

**HAL** is a multi-disciplinary open access archive for the deposit and dissemination of scientific research documents, whether they are published or not. The documents may come from teaching and research institutions in France or abroad, or from public or private research centers.

L'archive ouverte pluridisciplinaire **HAL**, est destinée au dépôt et à la diffusion de documents scientifiques de niveau recherche, publiés ou non, émanant des établissements d'enseignement et de recherche français ou étrangers, des laboratoires publics ou privés.

## **Carbonation of vegetable oils: influence of mass transfer on reaction kinetics**

**Jun L. Zheng<sup>1, 2</sup>, Fabrice Burel<sup>2</sup>, Tapio Salmi<sup>3</sup>, Bechara Taouk<sup>1</sup>, Sébastien**

**Leveueur<sup>1, 3\*</sup>**

1. Laboratoire de Sécurité des Procédés Chimiques (LSPC), EA4704, INSA de Rouen ,685 Avenue de l'université, BP 08, 76801 Saint-Etienne-du-Rouvray, France.

Tel: +33 2 32 95 66 54; Fax: +33 2 32 95 66 52; E-mail: sebastien.leveueur@insa-rouen.fr

2. Normandie Université, INSA de Rouen, PBS UMR 6270 FR 3038 CNRS, INSA de Rouen, 685 Avenue de l'Université, 76801 Saint Etienne du Rouvray, France;

3. Laboratory of Industrial Chemistry and Reaction Engineering, Johan Gadolin Process Chemistry Centre, Åbo Akademi University, Biskopsgatan 8, FI-20500 Åbo/Turku, Finland;

Keywords: carbonation of vegetable oils, optimization, CO<sub>2</sub> solubility, biomass valorization

### **Abstract**

The carbonation of epoxydized vegetable oil was studied by using tetra-n-butylammonium bromide (TBAB) as catalyst. Thermal stability of TBAB was studied by differential scanning calorimetry (DSC) and thermogravimetric analysis (TGA), and it was demonstrated that the maximum reaction temperature should not exceed 130°C. Reaction conditions were optimum at 130°C, 50 bar, with 3.5% mol of catalyst. The gas-liquid mass transfer coefficient and solubility of CO<sub>2</sub> were determined by taking into account the non-ideality of the gas phase using Peng-Robinson state equations. At 130°C, the CO<sub>2</sub> solubility was found to be independent from epoxide conversion and equal to 0.57 mol.L<sup>-1</sup>, and the gas liquid mass transfer

coefficient ( $k_{La}$ ) decrease with the epoxide conversion, i.e., at 0 % of conversion  $k_{La} = 0.0249 \text{ s}^{-1}$  and at 94 % of conversion  $k_{La} = 0.0021 \text{ s}^{-1}$ .

## 1. Introduction

The control of greenhouse gases, especially carbon dioxide, is one of the most serious challenges that humanity is facing today<sup>1,2</sup>. How the CO<sub>2</sub> molecule should be considered: waste or re-usable raw materials? Due to the difficulty to diminish the CO<sub>2</sub> emissions, the academic and industrial communities tend to recycle this molecule<sup>3</sup> in different ways such as the CO<sub>2</sub> storage, the use of CO<sub>2</sub> as solvent<sup>4</sup> or the use of CO<sub>2</sub> for enhanced oil recovery<sup>5</sup>. The benefit of these methods is the non-transformation of CO<sub>2</sub> but can it be a sustainable solution?

From a chemical viewpoint, carbon dioxide is considered as a C1 building block, i.e., synthesis of new molecules from a single-carbon molecule. Some industrial process exists such as the synthesis of urea or the synthesis of carbonated short-chain molecules. Investigation of direct synthesis of methanol from hydrogen and carbon dioxide is gaining growing interest. Private and public sectors are mobilized to develop the suitable catalyst, efficient chemical reactor and the cheapest non-fossil hydrogen in order to produce inexpensive methanol.

As summarized by Yu et al.<sup>6</sup> and Olajire<sup>7</sup>, there are other promising routes of CO<sub>2</sub> valorization into fuels such as formic acid, dimethyl carbonate, methyl formate or into chemicals such as carboxylates, lactones, carbamates, carboxylic acids or polymers.

These existing and potential industrial CO<sub>2</sub> valorization examples have shown the importance of kinetic, thermodynamic and mass transfer data. To be able to propose a sustainable process based on the CO<sub>2</sub> valorization, it is important to gather experimental data for the different routes of valorization.

The use of CO<sub>2</sub> as the raw material in an industrial park can ensure its sustainability. The philosophy of eco-park is to look for some renewable and inexpensive raw materials. The coupling of renewable materials and reusable materials could be of high interest from the viewpoint of economy and energy.

Vegetable oils (VOs) are excellent candidates for the substitution of petroleum-derived products due to their renewability, low toxicity and biodegradability<sup>8,9</sup>. The worldwide production of VOs for industrial use and as biodiesel components has increased in the past decades<sup>10</sup>. The research trend is to investigate different ways to modify VOs, and among them epoxidation and carbonation have received a lot of attention during the recent years<sup>11</sup>.

Synthesis of carbonated vegetable oils from epoxidized vegetable oils and carbon dioxide is a very green chemical route. Currently, carbonated vegetable oils are mainly used in the synthesis of nonisocyanate polyurethanes (NIPU), which does not require the use of highly toxic isocyanates compared with conventional methods<sup>12</sup>. They are also good candidates for lubricants to be used at high temperature and pressure<sup>11</sup>.

The atom economy of this reaction is close to 100%<sup>1,2</sup>. Indeed, carbon dioxide reacts with the epoxide group to produce cyclic carbonates (Figure 1).

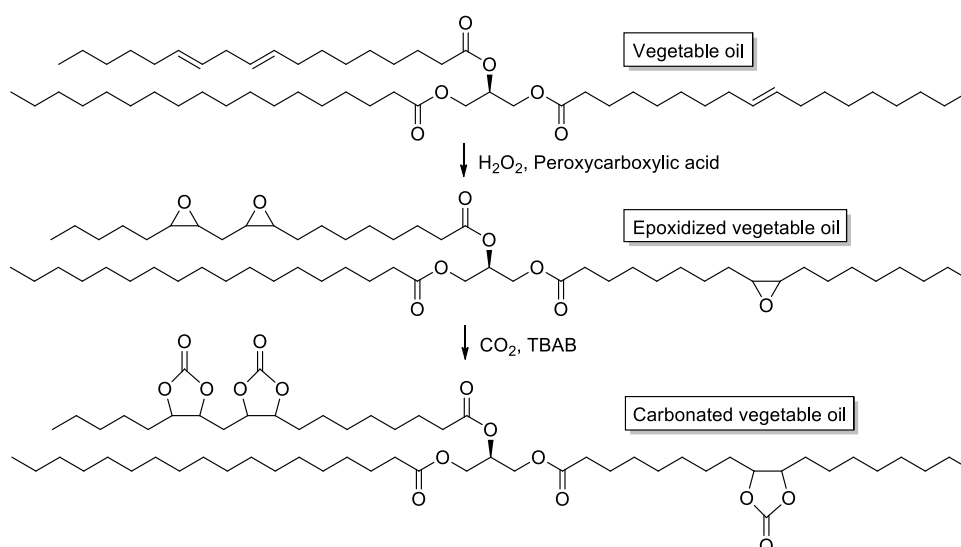


Figure 1. Synthesis of carbonated vegetable oils.

From a process point of view, the production of such compound should include the epoxidation process as illustrated by Figure 1. The epoxidation reaction is performed at atmospheric pressure by the Prileschajew reaction<sup>13</sup>. The carbonation reaction is performed at higher CO<sub>2</sub> pressure (50-70 bar) and temperature (140-150°C). Thus, these two steps cannot be performed in a one-pot synthesis.

Tamami et al.<sup>14</sup> were the first to publish the method of synthesis of carbonated soybean oil by using 5% of tetra-n-butylammonium bromide (TBAB) as catalyst under atmospheric pressure at 110°C. They have reported slow reaction rate and viscosity increased during this reaction. Experiment under same conditions were performed by Javni et al.<sup>15</sup> in 2008, 78% of conversion was achieved in 89 hours of reaction time.

In terms of catalysis, various co-catalysts such as SnCl<sub>4</sub>·5H<sub>2</sub>O<sup>16</sup> and CaCl<sub>2</sub><sup>17</sup> have been screened and enhanced the performance of TBAB. Other catalysts such as KI with 18-crown-6 ether (Parzuchowski et al.<sup>18</sup>, 2006), silica supported 4-pyrrolidinopyridinium iodide (Bähr et al.<sup>19</sup>, 2012), Pt doped H<sub>3</sub>PW<sub>12</sub>O<sub>40</sub>/ZrO<sub>2</sub> (Wang et al.<sup>20</sup>, 2012) have been tested, but they were less efficient.

In terms of process intensification, Doll et al.<sup>21</sup> have conducted the synthesis under supercritical CO<sub>2</sub>, achieving 94% of conversion, in 20 hours. Mazo et al.<sup>22</sup> have demonstrated that microwave irradiation improves the carbonation kinetics.

Table 1 summarizes the major results obtained for the carbonation of vegetable oils.

Table 1. General result obtained by various groups in carbonation of VO.

Reference	Oil	Nature of the reactor system	Catalyst
Tamami et al. <sup>14</sup>	ESBO	Flow of CO <sub>2</sub>	TBAB, homogeneous
Doll and Erhan <sup>21</sup>	ESBO	Autoclave/scCO <sub>2</sub>	TBAB, homogeneous
Parzuchowski et al. <sup>18</sup>	ESBO	Pressure reactor	KI/18-crown-6, homogeneous
Li et al. <sup>16</sup>	ESBO + DMF	Autoclave	TBAB/SnCl <sub>4</sub> , homogeneous
Javni et al. <sup>15</sup>	ESBO	Pressure reactor	TBAB, homogeneous
Wang et al. <sup>20</sup>	ESBO + DMF	Autoclave	H <sub>3</sub> PW <sub>12</sub> O <sub>40</sub> /ZrO <sub>2</sub> , heterogeneous
Bähr and Mülhaupt <sup>19</sup>	ELO	Pressure reactor	TBAB, homogeneous
Bähr and Mülhaupt <sup>19</sup>	ELO	Pressure reactor	(SiO <sub>2</sub> –(I)), heterogeneous
Mazo and Rios <sup>22</sup>	ESBO	Microwave irradiation with flow of CO <sub>2</sub>	TBAB, homogeneous
Zhang et al. <sup>23</sup>	ECSO	Autoclave	TBAB, homogeneous

\* ESBO: Epoxidized soybean oil; ELO: Epoxidized linseed oil; ECSO: Epoxidized cottonseed oil; SiO<sub>2</sub>–(I):silica-supported 4-pyrrolidinopyridinium iodide

Reference	Temperature [°C]	CO <sub>2</sub> pressure [Bar]	Reaction time [hours]	Conversion [%]
Tamami et al. <sup>14</sup>	110	1.01	70	94
Doll and Erhan <sup>21</sup>	100	103	20	94
Parzuchowski et al. <sup>18</sup>	130	6	48	98.3
Li et al. <sup>16</sup>	120	10	20	89.2
Javni et al. <sup>15</sup>	140	56.5	20	100
Wang et al. <sup>20</sup>	150	10	40	94.3
Bähr and Mülhaupt <sup>19</sup>	140	30	20	100
Bähr and Mülhaupt <sup>19</sup>	140	30	45	100
Mazo and Rios <sup>22</sup>	120	1.01	40	95
Zhang et al. <sup>23</sup>	140	30	24	100

TBAB is the most used catalyst for this reaction, but at higher temperature it can undergo decomposition into various products such as hydrogen bromide<sup>21</sup>.

To the best of our knowledge, no mass transfer studies have been performed on this reaction system. Knowing the mass transfer and mixing effects is however essential at the scale-up stage. Furthermore, as the double bond is saturated with steric chemical groups, the viscosity is expected to increase<sup>24</sup>. As described in the article of Campanella et al.<sup>24</sup>, epoxidized vegetable oils are non-Newtonian thixotropic fluids.

The main objective of this work was to study the limitation of different factors on the carbonation of epoxidized vegetable oils, and the kinetics of gas-liquid mass transfer by taking into account the non-ideality of the gas. Cottonseed oil was used during this study. The thermal stability of TBAB was investigated to determine its onset temperature of decomposition. A mass transfer study was performed by taking into account the non-ideality of the gas phase. Furthermore, a simple method was proposed to determine the solubility and mass transfer coefficient ( $k_{La}$ ) of CO<sub>2</sub> under non-ideal conditions, and the influence of temperature, addition of catalyst and epoxy group conversion was investigated.



## 2. Experimental part

### 2.1 Materials.

Cottonseed oil was purchased from Sigma-Aldrich Co., while hydrogen peroxide (33 wt % in water) and formic acid (99 wt %) was purchased from VWR International. Perchloric acid solution (0.1 M) in glacial acetic acid was purchased from Alfa Aesar GmbH. TBAB (99.8 wt %) was purchased from Alfa Aesar and carbon dioxide was purchased from Air Liquide.

### 2.2 Apparatus and experimental procedures.

Carbonation reaction and solubility measurements were carried out in a 300mL high-pressure stainless steel autoclave (Parr Instrument Company) shown in Figure 2. The reactor was equipped with a temperature control system. A pressure probe and a gas entrainment impeller (diameter 2.5 cm) with a hollow shaft were used. A gas feed system including a CO<sub>2</sub> bottle and a gas reservoir equipped with a pressure probe was connected to the reactor. The uncertainty for the pressure probe is 0.01 bar and for the temperature probe is 0.1°C.

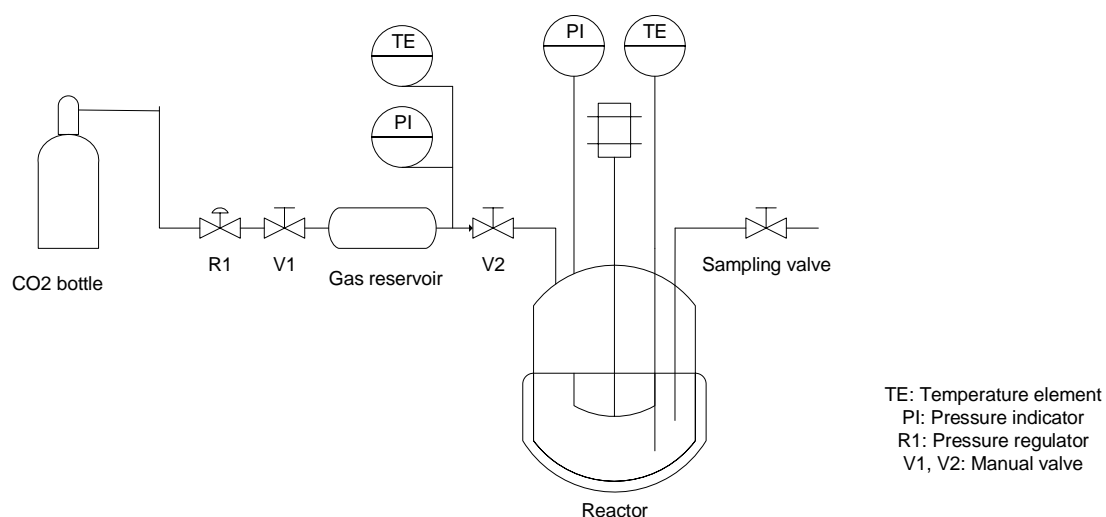


Figure 2. Simplified reactor scheme.

### **2.2.1 Preparation of epoxidized cottonseed oil.**

The epoxidized cottonseed oil (ECISO) was prepared according to the protocol described in our previous article<sup>25</sup>. 180 g of cottonseed oil, 180 g of hydrogen peroxide (33 wt %) and 50g of distilled water was loaded in a 500 mL glass-jacketed reactor and stabilized at 60°C under vigorous agitation, then formic acid was introduced via a dosing pump at a volumetric flow-rate of 2.9 ml/min for 25 minutes. The reaction took one hour after which the agitation was stopped for phase separation. The resulting aqueous phase was removed, and the organic phase was washed with 300 mL of a 10 wt % aqueous solution of Na<sub>2</sub>CO<sub>3</sub> in water, and three times with 200 mL of water to remove residual acid. The product was first dried using a rotary evaporator, and then magnesium sulfate was added to further remove water present in the product. The final product was filtered and stored at 3°C under argon to prevent oxidation. The epoxide content was measured by the method of Jay<sup>26</sup>, and the conversion of double bounds was characterized by titrating the iodine value using the method of Hanus<sup>27</sup>. The resulting epoxidized cottonseed oil had a conversion exceeding 97% and the selectivity exceeded 81%.

### **2.2.2 Kinetic study of carbonation reaction.**

The epoxidized cottonseed oil and the catalyst (TBAB) were charged into the reactor and heated to the desired temperature under agitation. Then, the agitation was stopped and the atmosphere inside the reactor was purged with CO<sub>2</sub>. The output pressure was adjusted via the pressure regulator R1 connected to the CO<sub>2</sub> bottle, then valve V2 was opened and the stirring was started at the desired speed. Samples were withdrawn via the sampling valve during the reaction, and stored at 3°C prior to analysis.

### **2.2.3 Measurement of CO<sub>2</sub> solubility.**

Epoxidized cottonseed oil (with or without catalyst) was charged into the reactor and heated to the desired temperature under agitation, then the agitation was stopped and the atmosphere inside the reactor was purged with CO<sub>2</sub>. Using the regulator R1, CO<sub>2</sub> was introduced into the gas reservoir at the desired pressure. After the pressure stabilization, the agitation was switched on. The pressure and temperature in the gas reservoir were monitored in order to obtain the amount of CO<sub>2</sub> dissolved in the liquid phase.

### **2.3 Analytical methods.**

The concentration of the oxirane group was determined by the method of Jay, where oil samples were dissolved in a solution of 10 ml tetra-n-etylammonium bromide (20 w% ) and 10 ml of chloroform, then titrated by using a 0.1 N perchloric acid solution in acetic acid<sup>26</sup>. The uncertainty of the titration method is 0.01mol/L. The structure of products was characterized by Fourier transform infrared (FTIR) (Perkin-Elmer), <sup>1</sup>H NMR and <sup>13</sup>C NMR (Bruker Avance 300 MHz Spectrometer). Studies on the thermal stability of products were carried out using TA Instruments Q1000 Modulated Differential Scanning Calorimeter (DSC) and Q600 thermogravimetric analysis (TGA). For the DSC, temperature and energy calibration were performed using indium ( $T_{\text{fusion}} = 156.6^{\circ}\text{C}$  et  $\Delta H_{\text{fusion}} = 28.45 \text{ J.g}^{-1}$ ). Samples were heated from  $-90^{\circ}\text{C}$  to  $100^{\circ}\text{C}$  under nitrogen ( $50 \text{ mL.min}^{-1}$ ) using a heating rate of  $10^{\circ}\text{C/min}$ . For the TGA, calibration was performed using Alumel and Nickel which Curie points are respectively  $163^{\circ}\text{C}$  and  $358^{\circ}\text{C}$ .

Dynamic viscosity of cottonseed oil (CSO), epoxidized cottonseed oil (ECSO) and carbonated cottonseed oil (CCSO) were measured with the viscometers FUNGILAB.S.A and BROOKFIELD CAP2000+.

### 3. Results and discussions

#### 3.1 Thermal stability of catalyst

At high temperature, TBAB can readily decompose into volatile and toxic compounds such as Hydrogen Bromide<sup>21</sup> (Figure 3), which is highly reactive with epoxy groups. To prevent the decomposition of TBAB and potential side reactions, the carbonation reaction should be carried out at a temperature lower than the TBAB decomposition temperature. For this purpose, a decomposition study by DSC and TGA analysis was performed.

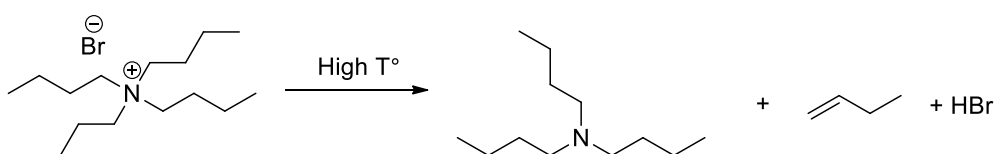


Figure 3. Decomposition of TBAB

Figure 4 shows the TBAB thermogram under dynamic mode from 50°C to 250°C with a temperature ramp of 1°C/min. One can notice the presence of two peaks at 86°C and 116°C, which corresponds respectively to crystalline structure and phase change<sup>28</sup>. The third peak corresponds to the TBAB decomposition, but due to the difficulty of determining the onset temperature under DSC, studies with TGA was carried out.

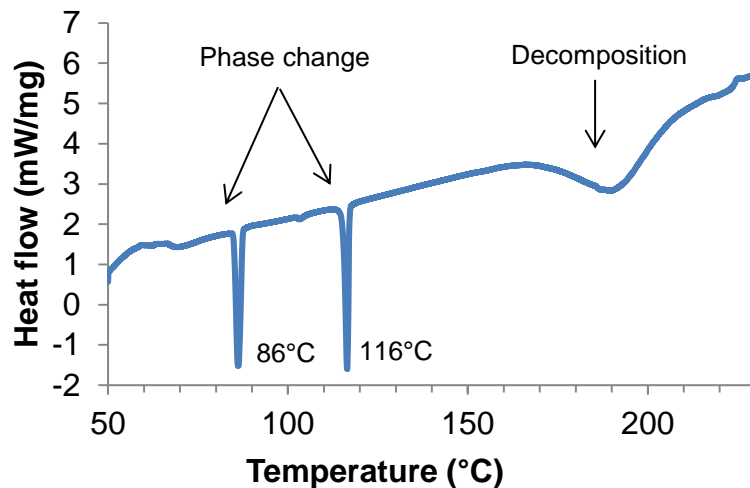


Figure 4. Dynamic thermal analysis of TBAB by DSC under dynamic mode with a heating ramp of 1°C/min.

Sample was heated under dynamic mode from 50°C to 300°C with a temperature ramp of 2°C/min. Starting of the mass drop was observed at ca.130°C (Figure 5).

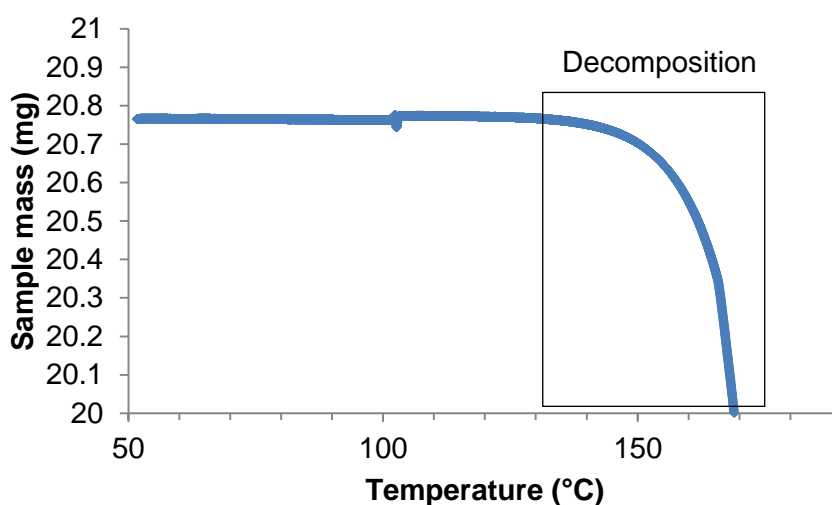


Figure 5. Dynamic thermal analysis of TBAB by TGA under dynamic mode with a heating ramp of 2°C/min.

To verify the stability of TBAB on a long reaction time, TGA experiments under isothermal mode at 120°C, 130°C, 140°C and 150°C were conducted for 10 hours (Figure 6).

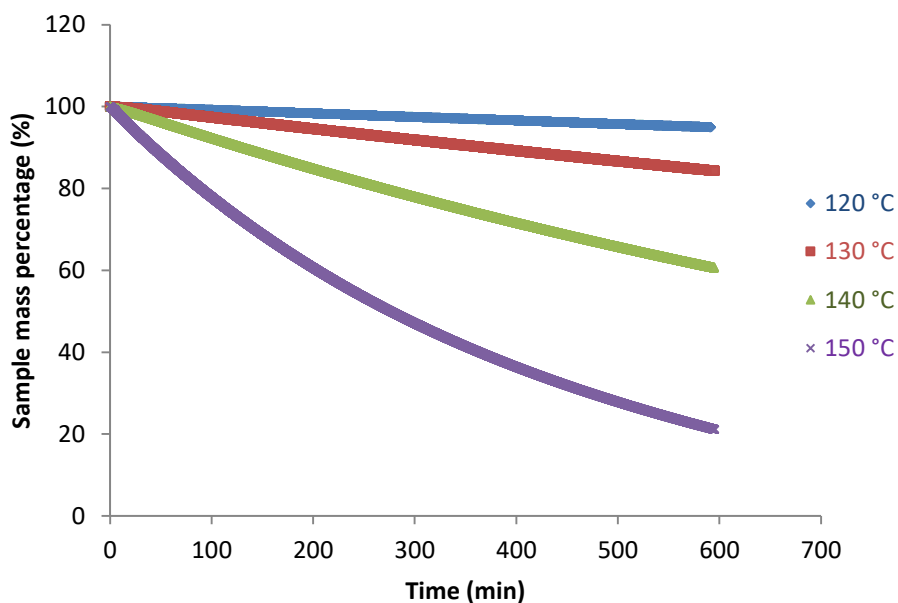


Figure 6. Study of TBAB thermal stability under isothermal mode by TGA.

It can be noticed that at 140°C and 150°C, the mass loss of TBAB is significantly faster and higher than at 120°C and 130°C. Thus, carbonation experiments should be performed at reaction temperature lower than 130°C to prevent catalyst loss.

One should also keep in mind that experiments carried out in DSC or TGA were not performed in similar condition as the one in the autoclave. Indeed, during the micro-calorimetry experiments, there was not epoxidized cottonseed oil and CO<sub>2</sub> atmosphere, which could interfere slightly with the onset temperature.

### 3.2 Influence of rotation speed.

To check the influence of the agitation velocity on the reaction kinetics, experiments were carried out at different rotating speeds (300-900 rpm), at 130°C, 50 bar of CO<sub>2</sub> pressure and with 3.5 mol% of TBAB with respect to epoxy groups (Figure 7). One can distinguish two different behaviors: low rotating speed, i.e. < 300 rpm and high rotating speed, i.e., > 500 rpm. Rate of ECSO conversion is lower for experiments carried out at 300 rpm during 400 minutes of reaction time, which can be linked to a

slow gas-liquid mass transfer rate. Experiments carried out at 500, 700 or 900 rpm show similar kinetics. Thus, to optimize the rate of ECSO conversion, experiments were carried out at 500 rpm.

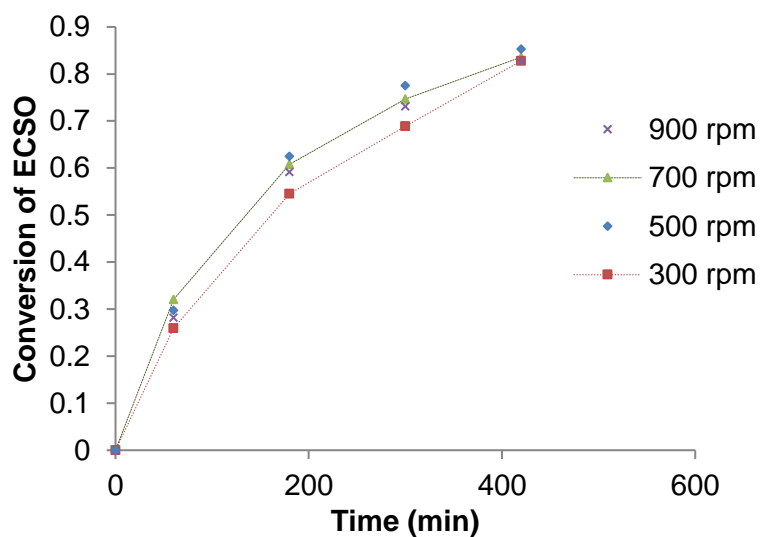


Figure 7. Influence of rotation speed on ECSO conversion at 130°C.

### 3.3 Influence of catalyst loading.

The carbonation reaction was studied with 1.4, 3.5, 5 and 10 mol% of TBAB with respect to the epoxide groups (Figure 8). As there is no significant kinetic increase from 3.5% to 5% of catalyst and 10% was impractical in real situations, 3.5% TBAB have been chosen for the rest of this work.

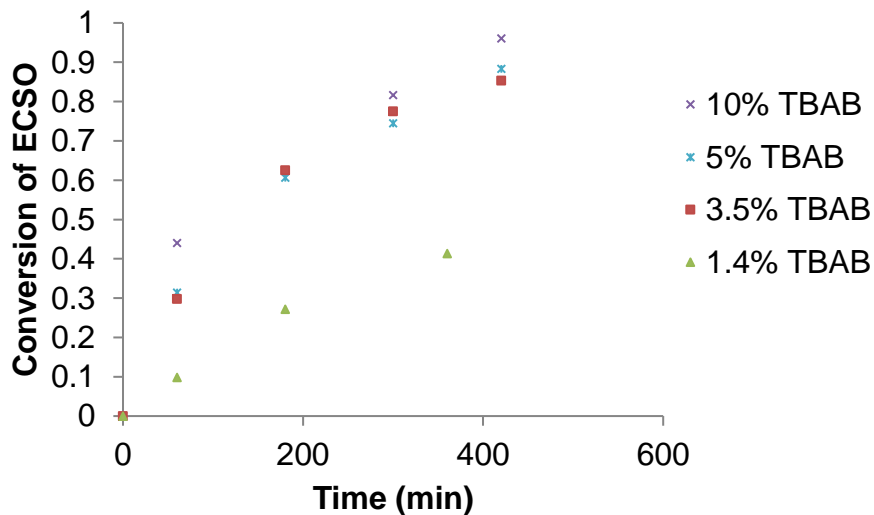


Figure 8. Influence of catalyst amount on reaction kinetics at 130°C, 50 bar and 500 rpm.

### 3.4 Influence of temperature and CO<sub>2</sub> pressure.

The kinetic study was studied within the temperature range of 110-130°C for the sake of catalyst stability and within the CO<sub>2</sub> pressure range of 30-50 bar (Figures 9-10).

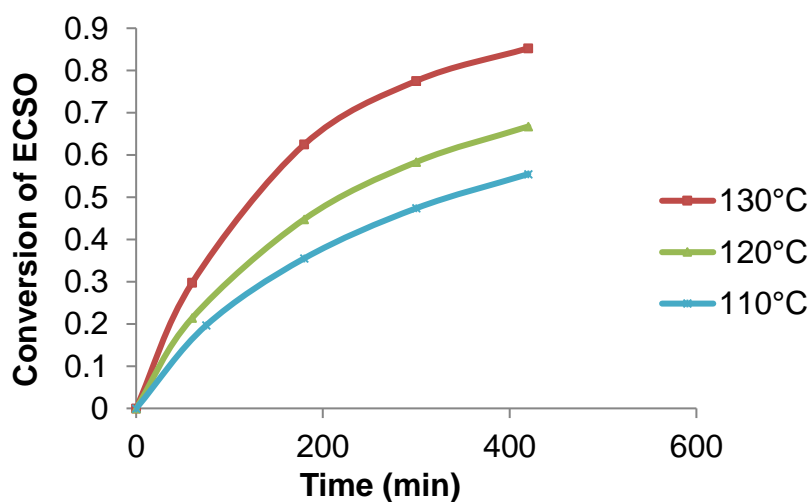


Figure 9. Influence of temperature on reaction kinetics at 50 bar and with 3.5 mol% TBAB at 500 rpm.



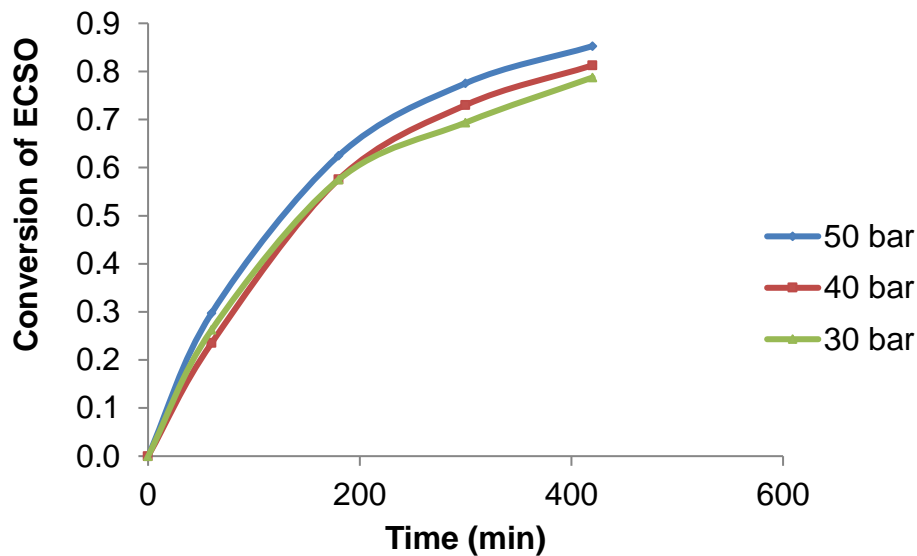


Figure 10. Influence of CO<sub>2</sub> pressure on reaction kinetics at 130°C, with 3.5 mol% TBAB at 500 rpm.

Figure 9 shows that as the reaction temperature increases, the initial rate of ESCO conversion increase. The increase of reaction temperature leads to the increase of carbonation reaction kinetics with Arrhenius law and the increase of mass transfer kinetics which is proportional to the temperature<sup>29</sup>.

From Figure 10, it can be noticed that initial kinetics between 30 and 50 bar of CO<sub>2</sub> was not significantly different. One could have expected that by increasing the CO<sub>2</sub> pressure, carbonation reaction kinetic could have been higher due to a faster mass transfer linked to a higher CO<sub>2</sub> gradient. In this system, there is slight benefit to increase the CO<sub>2</sub> pressure on reaction temperature within reaction pressure of 30-50 bar. Bähr and Mülhaupt<sup>19</sup> have noticed that the conversion of epoxidized linseed oil a 140°C have a stronger influence on reaction kinetics between 1 atm and 10 bar than between 10 and 30 bar.

Based on the thermal study of the catalyst, the influence of the catalyst amount and CO<sub>2</sub> pressure, it can be stated that the optimal experimental conditions were 130°C, 50 bar of CO<sub>2</sub> and 3.5 mol % of TBAB.

### 3.5 Product characterization.

Samples withdrawn at different reaction times during the reaction were analyzed by <sup>1</sup>H NMR, <sup>13</sup>C NMR and FTIR. Figure 11 clearly reveals the formation of carbonyl groups on the band 1800 cm<sup>-1</sup> and the consumption of oxirane groups in the wavenumber range of 820-840 cm<sup>-1</sup>.

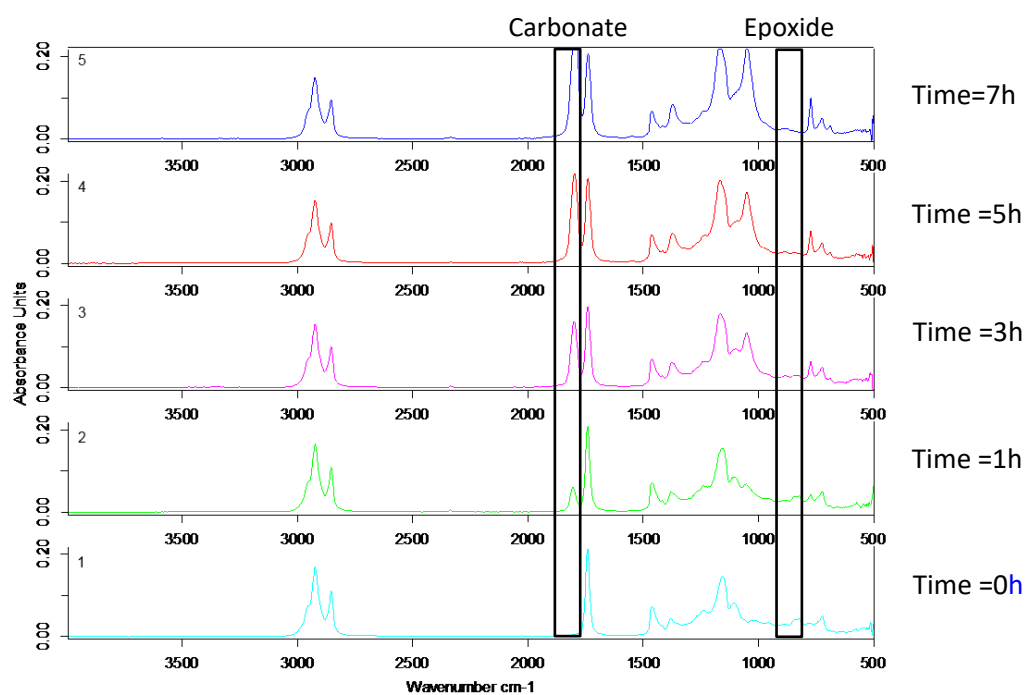


Figure 11. FTIR spectra for samples at different reaction times at 130°C, 50 bar and 3.5 mol% of TBAB under 500 rpm.

Figure 12 shows the <sup>1</sup>H NMR spectra of the same sample as on FTIR. Epoxy groups towards 2.8-3.1 ppm decreased during the reaction and carbonates at 4.3-4.9 ppm were formed. By taking the group at 4.09-4.15 ppm as reference (two protons from

glycerol), the integration can be normalized and the selectivity of the reaction can be calculated by

$$S (\%) = \frac{C - 2}{A - B} = \frac{8.11 - 2}{6.55 - 0.21} = 0.96$$

where A is the integration of signal of sample 1 from 2.8 to 3.1 ppm (initial amount of epoxide), B the integration of signal of sample 5 from 2.8 to 3.1 ppm (final amount of epoxide), and C the integration of signal of sample 5 from 4.2 to 4.9 ppm (signal of carbonates with 2 protons from glycerol). The final value obtained for these conditions is 96%.

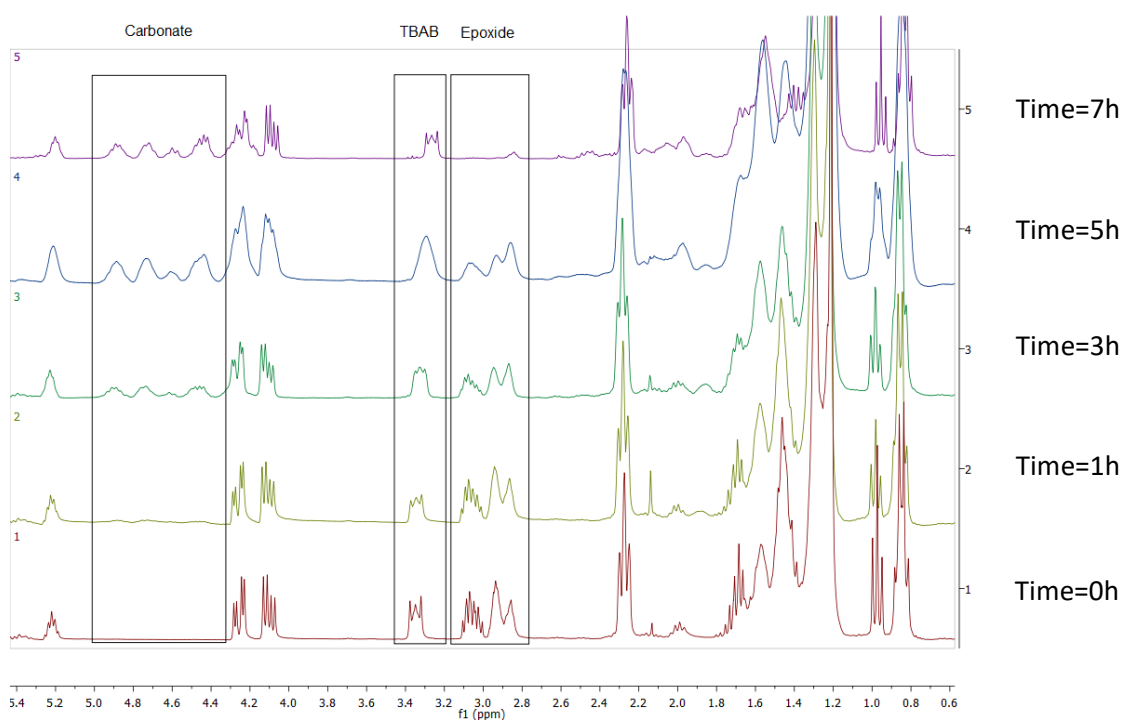


Figure 12.  $^1\text{H}$  NMR spectra for samples at different intervals of reaction.  $T= 130^\circ\text{C}$ ,  
 $P=50\text{bar}$ , 3.5% TBAB.

Furthermore,  $^{13}\text{C}$  NMR spectra were obtained for the initial (1) and final (2) products. The signals of oxirane groups are located at 54.4, 56.8, 57.1, 57.3 ppm, and signals of carbonates are located at 77.8, 79.5, 82.1 and 153.9 ppm (Figure 13).

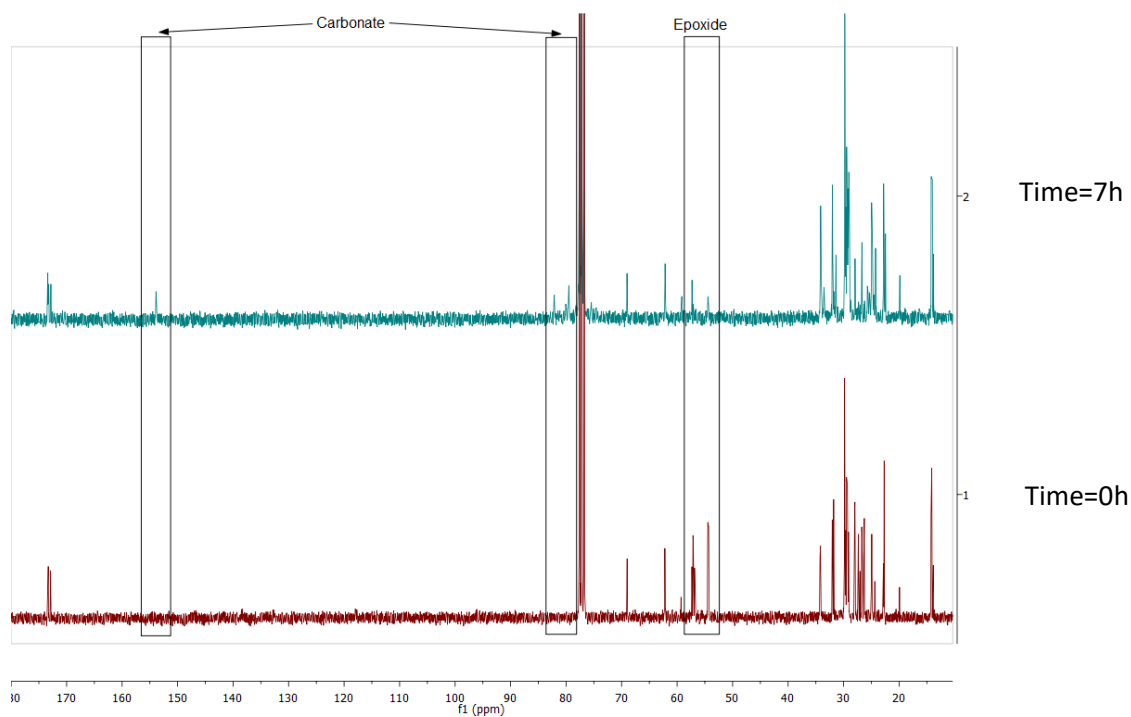


Figure 13.  $^{13}\text{C}$  NMR spectra for samples at the beginning (1) and the end (2) of reaction.  $T=130^\circ\text{C}$ ,  $P=50\text{bar}$ , 3.5% TBAB.

### 3.6 Measurement of CO<sub>2</sub> solubility.

The concentration of CO<sub>2</sub> present in the liquid phase is an important factor affecting the reaction kinetics. For this reason, the evolution of this factor with the conversion of ECSO and the influence of the electrolyte TBAB was investigated. Indeed, Henry's coefficient and mass transfer parameters might change with the reactant conversion due to the increase of the liquid viscosity. Figure 14 illustrates this evolution.

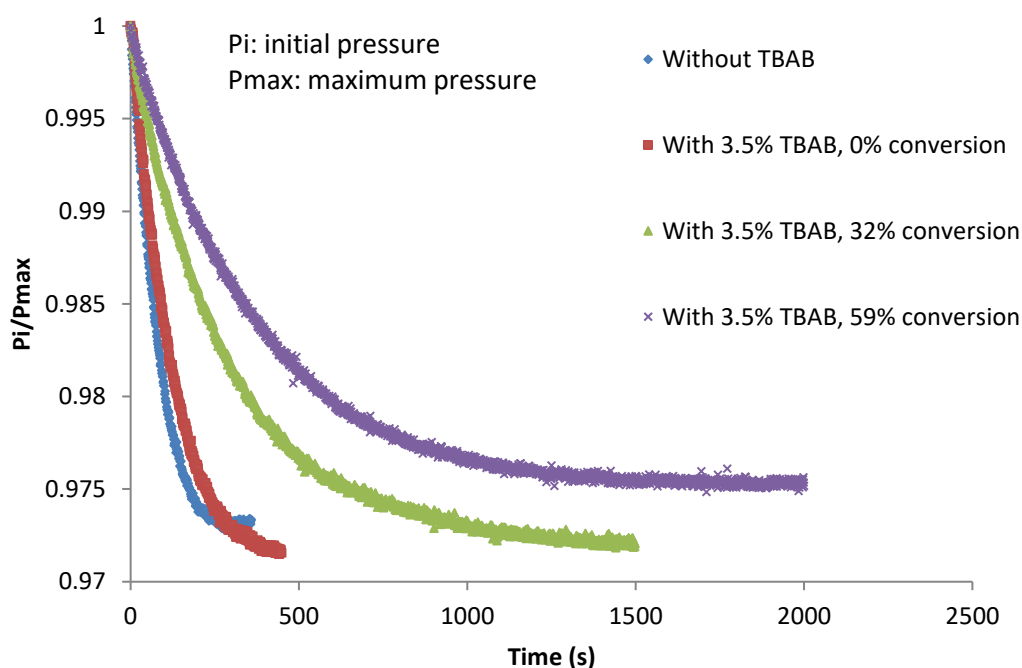


Figure 14. Normalized pressure drop rate at 100°C, with and without catalyst and at different ECSO conversions.

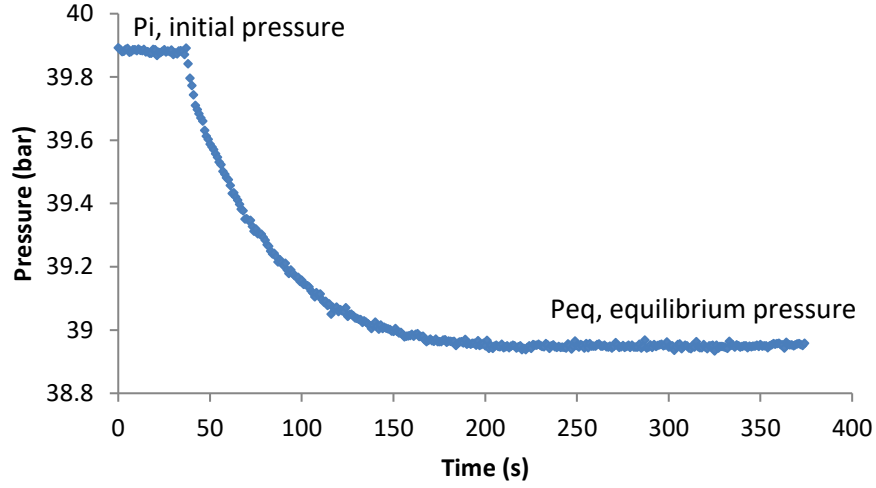


Figure 15. Pressure drop in the gas reservoir at 120°C in absence of TBAB.

As shown in Figure 15, the pressure drop was monitored, the initial pressure ( $P_i$ ) and equilibrium pressure ( $P_{eq}$ ) was used to calculate the amount of  $CO_2$  dissolved in the oil. In the presence of the catalyst, the carbonation reaction occurs simultaneously with  $CO_2$  absorption and increases the pressure drop in the reactor. In order to surmount this problem, the pressure was interpolated to determine the corresponding equilibrium pressure.

The reactor and gas reservoir were considered as two individual parts stabilized at the same pressure at different temperatures  $T_r$  and  $T_{res}$ , respectively. Due to the non-ideality of  $CO_2$  at high pressure, the Peng-Robinson state equation was used to calculate the compressibility factor  $Z^{30}$ :

$$P = \frac{RT}{\frac{V}{n_{CO_2}} - b} - \frac{a(\omega, T_r)}{\frac{V}{n_{CO_2}} \left( \frac{V}{n_{CO_2}} + b \right) + b \left( \frac{V}{n_{CO_2}} - b \right)} \quad (1)$$

with

$a(\omega, T_r) = a_c \alpha(\omega, Tr)$ , where  $\omega$  is the acentric factor and  $Tr$  is the reduced temperature defined as  $T/T_c$ ;

$a_c = \frac{0.45724R^2T_c^2}{P_c}$ , where  $T_c$  and  $P_c$  are temperature and pressure at CO<sub>2</sub> critical

point respectively,

$$\alpha(\omega, T_r) = \left(1 + \kappa(1 - \sqrt{T_r})\right)^2,$$

$$\kappa = 0.37464 + 1.54226\omega - 0.26992\omega^2$$

$$b = \frac{0.07780RT_c}{P_c}.$$

Equation (1) can be put in polynomial form as:

$$Z^3 - (1 - B).Z^2 + (A - 2.B - 3.B^2)Z - (A.B - B^2 - B^3) = 0 \quad (2)$$

with:

$$A = \frac{a.\alpha.P}{R^2T^2},$$

$$B = \frac{b.P}{R T},$$

$$Z = \frac{P.V}{n_{CO_2}R.T}.$$

The cubic equation (2) was solved by Newton-Raphson method in order to obtain the compressibility factor  $Z$ .

Thus the quantity of CO<sub>2</sub> at the beginning and at equilibrium can be calculated by the following equations:

$$n_{g,i} = n_{r,i} + n_{res,i} = \frac{P_i(V_r - V_L)}{Z_r R T_r} + \frac{P_i V_{res}}{Z_{res} R T_{res}} \quad (3)$$

$$n_{g,eq} = n_{r,eq} + n_{res,eq} = \frac{P_{eq}(V_r - V_L)}{Z_r R T_r} + \frac{P_{eq} V_{res}}{Z_{res} R T_{res}} \quad (4)$$

Table 2 presents some values of  $Z_r$  and  $Z_{res}$ . In the reservoir the value of the compressibility factor is close to 0.7, and in the reactor the compressibility factor is ca. 0.9. These values are lower than 1 showing the non-ideality of the gas phase.

The concentration of  $CO_2$  in the oil at  $T_r$  and  $P_{eq}$  can be expressed as

$$C_{CO_2} = \frac{n_i - n_{eq}}{V_{oil}} \quad (5)$$

The Henry's constant can be calculated from

$$k_{H,CO_2} = \frac{P_{eq}}{C_{CO_2}} \quad (6)$$

Table 2 shows the solubility data within the temperature range 100-130°C. The solubility of  $CO_2$  in the epoxidized or carbonated cottonseed oil is similar and there are no significant changes in solubility by the addition of TBAB. The  $CO_2$  solubility decrease when temperature increases, which is a classical behavior.

### 3.7 Measurement of mass transfer coefficients.

To measure mass transfer coefficient, we have followed the variation of pressure as in the work of Laugier<sup>31</sup>, Frikha<sup>32</sup> and Hichri<sup>33</sup>. The mass transfer coefficient ( $k_L a$ ) is defined by the following equation:

$$-\frac{dn_g}{dt} = V_L k_L a (C_L^* - C_L) \quad (7)$$

By assuming that the liquid phase volume is constant, Eq. (7) becomes

$$-\frac{dn_g}{dt} = V_L k_L a \left( \frac{n_{CO_2,L,eq}}{V_L} - \frac{n_{CO_2,L}}{V_L} \right) \quad (8)$$

$$= k_L a [(n_{g,i} - n_{g,eq}) - (n_{g,i} - n_{g,t})]$$



Where  $n_{g,t}$  represents the amount of  $\text{CO}_2$  molecules at time  $t$ ,  $n_{g,i}$  the initial amount of  $\text{CO}_2$  molecules and  $n_{g,eq}$  the amount of molecules at the equilibrium.

Integration of Eq. (8) gives

$$\int_{n_{g,i}}^{n_{g,t}} \frac{dn_{g,t}}{n_{g,eq} - n_{g,t}} = k_L a \cdot \int_{t_0}^t dt \quad (9)$$

which is equivalent to

$$\ln \left( \frac{n_{g,eq} - n_{g,t}}{n_{g,eq} - n_{g,i}} \right) = k_L a \cdot (t - t_0) \quad (10)$$

By plotting  $\ln \left( \frac{n_{g,f} - n_{g,t}}{n_{g,f} - n_{g,i}} \right)$  along the time  $t$ ,  $k_L a$  can be estimated. Measurements were performed in the temperature range of 100-130°C and graphical results are displayed in Figures 16-19.

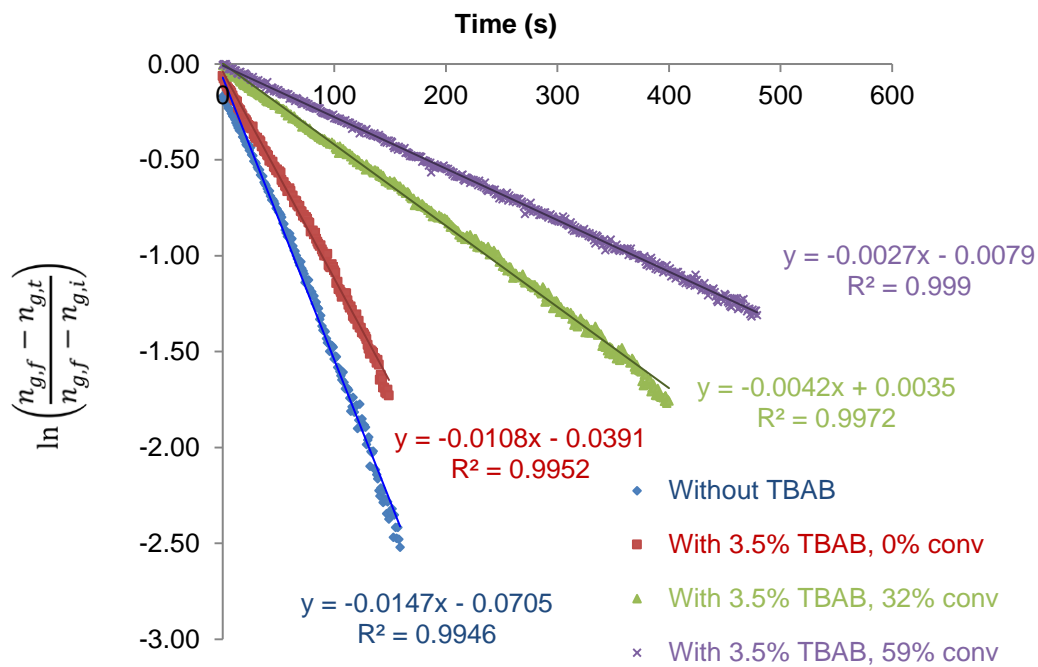


Figure 16. Mass transfer coefficient plot at 100°C.

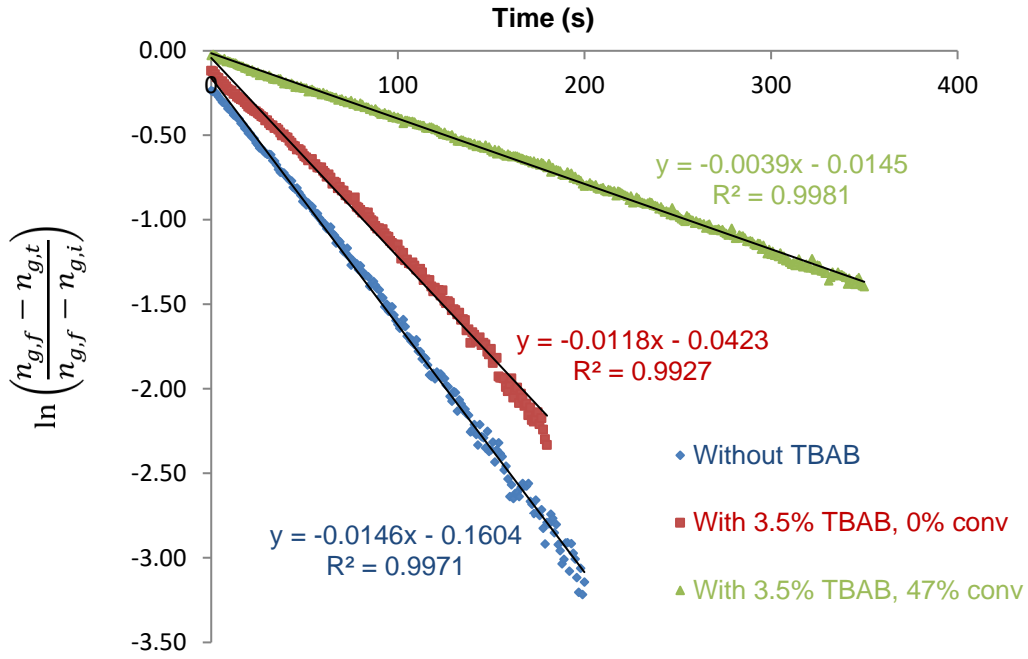


Figure 17. Mass transfer coefficient plot at 110°C.

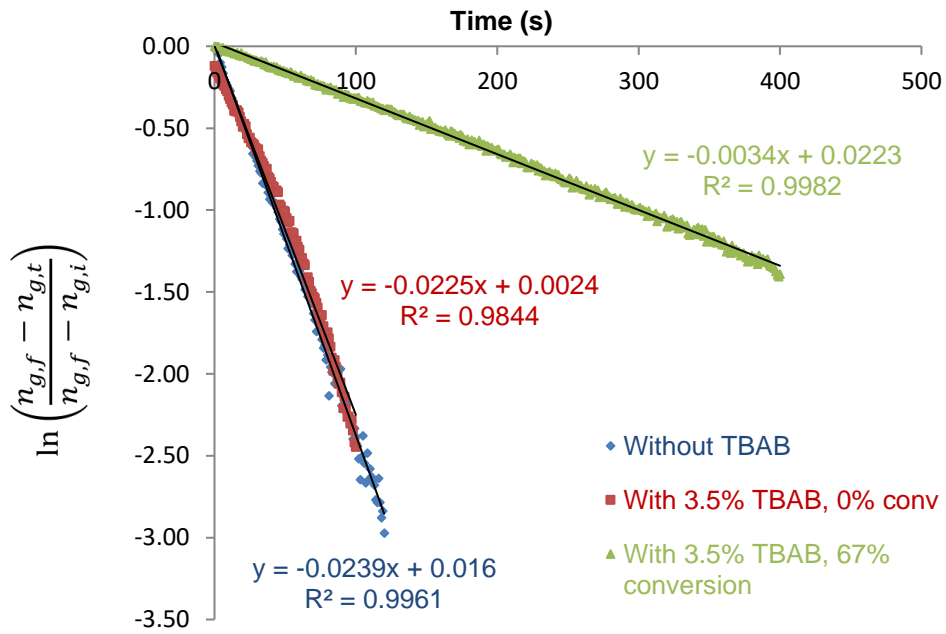


Figure 18. Mass transfer coefficient plot at 120°C.

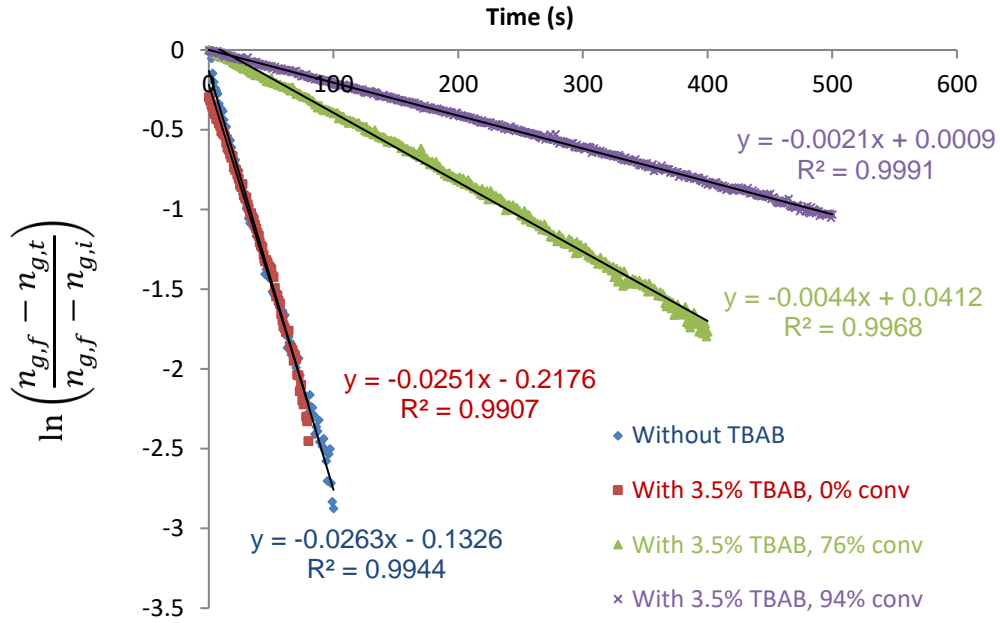


Figure 19. Mass transfer coefficient plot at 130°C.

The correlation developed by Kawase and Moo-Young<sup>34</sup> relates the mass transfer coefficient to liquid viscosity:

$$k_{Liq} \cdot a = \frac{2}{\sqrt{\pi}} \sqrt{D_{CO_2/Liq}} \left( \frac{\xi \cdot \rho^{Liq}}{\mu^{Liq}} \right)^{1/4} \cdot a \quad (11)$$

Carbonated cottonseed oil (CCSO) has a higher viscosity than the epoxidized cottonseed oil<sup>24</sup>. From Eq. (11), as the conversion of ECSO increases, then the volumetric mass transfer coefficient decreases. This tendency was observed with the experimental data (Figure 20).

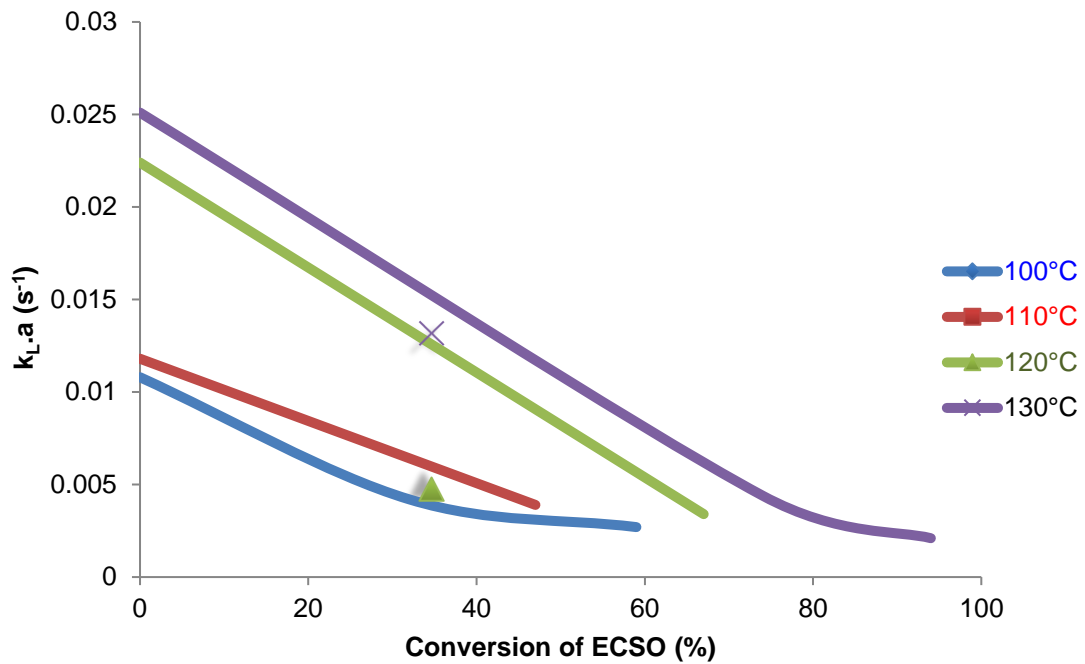


Figure 20. Mass transfer coefficients with ECSO conversion with 3.5 mol% of TBAB at different reaction temperature.

It can be noticed that as the reaction temperature increases, the volumetric mass transfer coefficient increases (Figure 20).

From Table 2, the addition of TBAB decreased  $k_{L,a}$  by about  $\frac{1}{4}$  at 110°C and below, but this phenomenon is not as evident at 120°C and 130°C. This is possibly due to the phase change of TBAB at 116°C, observed on the DSC graph (Figure 4). Table 2 summarizes the CO<sub>2</sub> solubility data and the values of the volumetric mass transfer coefficient,  $k_{L,a}$ .

Table 2. Solubility of CO<sub>2</sub> and gas-liquid mass transfer coefficients under various conditions.

T <sub>r</sub> (°C)	Pressure (bar)	[TBAB] (mol%)	Epoxide conversion (%)	Z <sub>res</sub>	Z <sub>r</sub>	CO <sub>2</sub> solubility (mol·L <sup>-1</sup> )	k <sub>La</sub> (s <sup>-1</sup> )	k <sub>H,CO2</sub> (L·bar·mol <sup>-1</sup> )
100	39.89	-	0	0.70	0.89	0.66	0.0147	60.44
100	40.05	3.5	0	0.70	0.89	0.65	0.0108	61.62
100	41.62	3.5	32	0.69	0.89	0.66	0.0043	63.06
100	40.04	3.5	59	0.69	0.89	0.67	0.0027	59.76
110	40.10	-	0	0.70	0.90	0.59	0.0145	67.97
110	40.08	3.5	0	0.70	0.90	0.61	0.0117	65.70
110	41.65	3.5	47	0.69	0.90	0.64	0.0040	65.08
120	39.65	-	0	0.70	0.91	0.53	0.0238	74.81
120	39.95	3.5	0	0.70	0.91	0.60	0.0224	66.58
120	42.35	3.5	67	0.68	0.91	0.51	0.0036	83.04
130	41.88	-	0	0.68	0.92	0.57	0.0262	73.47
130	41.00	3.5	0	0.68	0.92	0.55	0.0249	74.55
130	42.05	3.5	74	0.68	0.92	0.57	0.0046	73.77
130	44.30	3.5	94	0.67	0.91	0.59	0.0021	75.08

### 3.8 Measurement of viscosity

We have measured the viscosity of cottonseed oil, epoxidized cottonseed oil and carbonated cottonseed oil (Figure 21). One can notice that the viscosity of carbonated cottonseed oil (CCSO) is higher than the epoxidized (ECSO) and vegetable oil (CSO). However, as the temperature increase, the difference of viscosity between these different species is less pronounced.

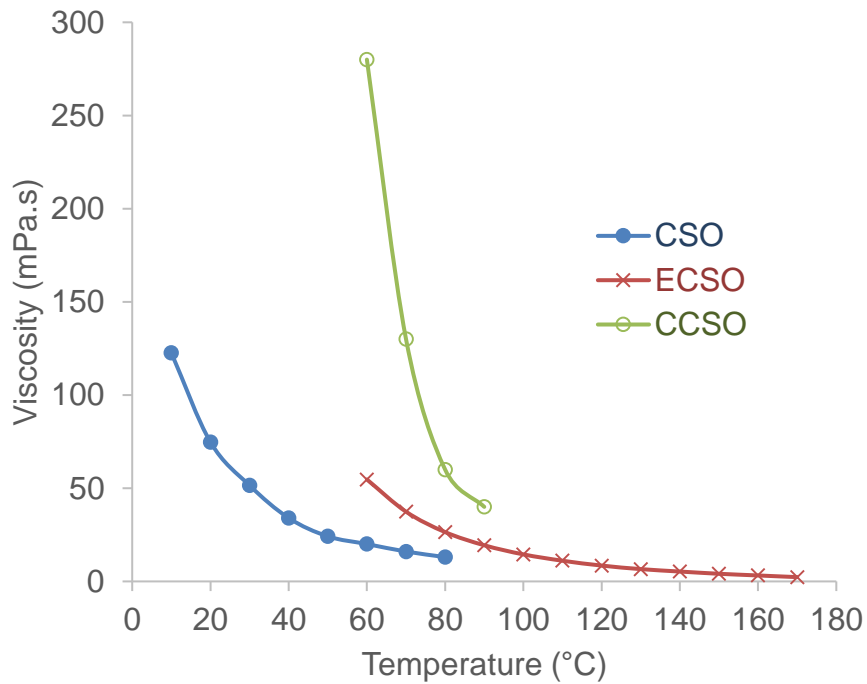


Figure 21. Dynamic viscosity of the different vegetable oils.

Zhang et al.<sup>23</sup> have measured the kinetic viscosity at different conversion of ECSO at 40 and 100°C. To compare their results with our results, we have assumed that densities of CSO, ECSO and CCSO are similar and equal to 1000 kg.m<sup>-3</sup>. Figure 22 shows the evolution of dynamic viscosity with the conversion of ECSO. One can notice that at 100°C, the dynamic viscosity of ECSO and CCSO is respectively, 14.3 mPa.s and 64.7 mPa.s. As the viscosity increases during the reaction, gas-liquid mass transfer coefficient (Eq. (11)) decreases.

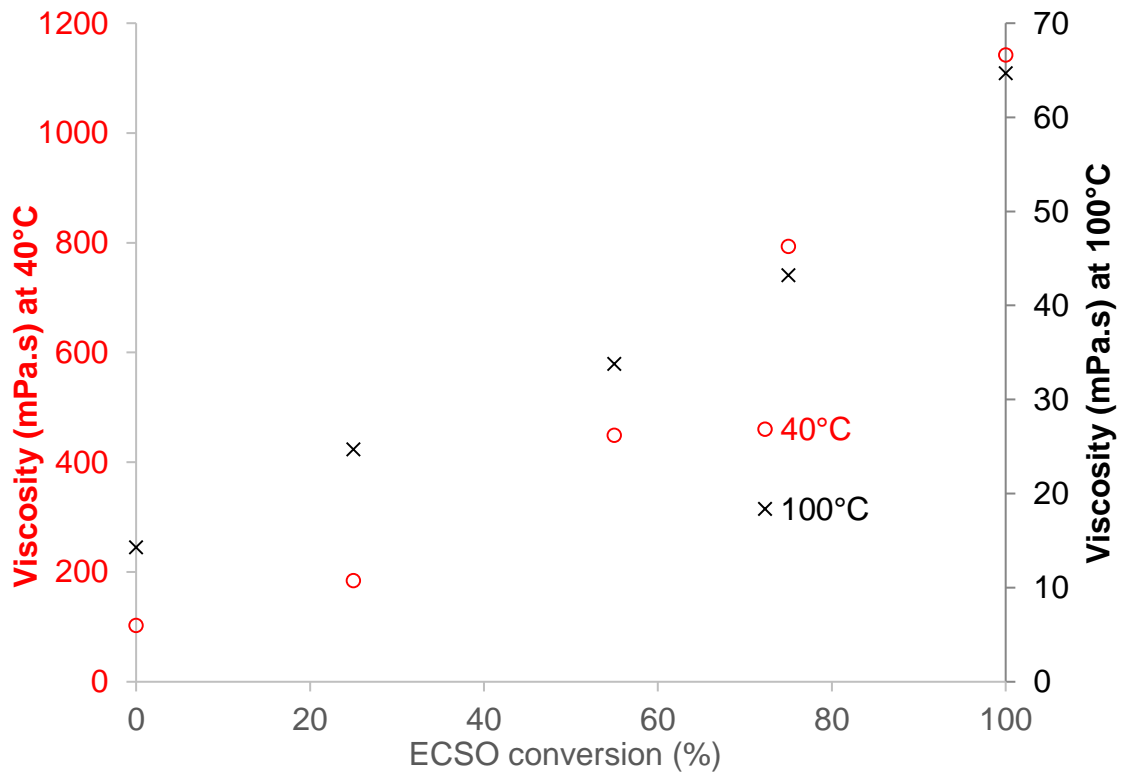


Figure 22. Evolution dynamic viscosity with ECSO conversion at 40 and 100°C.

#### 4 Conclusions

The carbonation of epoxidized cottonseed oil using TBAB as the catalyst has been studied in the temperature range of 110-130°C, and in the pressure range of 30-50 bars. NMR and FTIR analytic techniques were used to determine the presence of carbonated cottonseed oil.

The catalyst onset temperature was found to be at ca. 130°C. The optimal reaction condition was determined to be 130°C and 50 bar of CO<sub>2</sub> pressure. The conversion and selectivity were 85 % and 96 %, respectively for seven hours of reaction.

Mass transfer coefficient of CO<sub>2</sub> was found to decrease with the epoxide conversion due to an increase of viscosity. For example, at 130°C, mass transfer coefficient was measured to 0.0249 s<sup>-1</sup> at 0% of epoxide conversion and to 0.0021 s<sup>-1</sup> at 96 % of epoxide conversion.

Solubility of CO<sub>2</sub> was independent of epoxide conversion and decrease with increasing reaction temperature. For example, at 100°C the solubility was calculated to 0.65 mol.L<sup>-1</sup> and at 130°C the solubility was 0.55 mol.L<sup>-1</sup>.



## Nomenclature

$T_r$ (°C)	Reactor temperature
$T_a$ (°C)	Ambient temperature
$P_i$ (bar)	Initial pressure
$P_{eq}$ (bar)	Equilibrium pressure
$V_r$ (L)	Volume of reactor
$V_{res}$ (L)	Volume of gas reservoir
$V_L$ (L)	Volume of liquid phase
$n_{g,i}$ (mol)	Total initial molar molar quantity of CO <sub>2</sub> in the gas phase
$n_{g,eq}$ (mol)	Total molar molar quantity of CO <sub>2</sub> in the gas phase at equilibrium
$n_{r,i}$ (mol)	Initial molar molar quantity of CO <sub>2</sub> in the reactor
$n_{r,eq}$ (mol)	Molar molar quantity of CO <sub>2</sub> in the reactor at equilibrium
$n_{res,i}$ (mol)	Initial molar molar quantity of CO <sub>2</sub> in the gas reservoir
$n_{res,eq}$ (mol)	Molar molar quantity of CO <sub>2</sub> in the gas reservoir at equilibrium
$Z_r$	Compressibility factor of CO <sub>2</sub> in the reactor
$Z_{res}$	Compressibility factor of CO <sub>2</sub> in the gas reservoir
$k_L \cdot a$ (s <sup>-1</sup> )	Gas-liquid mass transfer coefficient
$k_{H,CO_2}$ (L·bar·mol <sup>-1</sup> )	Henry's constant
$C_L^*$ (mol·L <sup>-1</sup> )	Concentration of CO <sub>2</sub> in the liquid phase at equilibrium
$C_L$ (mol·L <sup>-1</sup> )	Concentration of CO <sub>2</sub> in the liquid phase at time t
$D_{CO_2/Liq}$ (m <sup>2</sup> ·s <sup>-1</sup> )	Diffusion coefficient of CO <sub>2</sub> in the liquid phase
$\xi$ (W·kg <sup>-1</sup> )	Energy dissipation rate per unit mass
$\mu_L$ (Pa·s)	Liquid viscosity

## **Acknowledgments**

The authors express their gratitude to Bruno Daronat and Christine Devouge-Boyer for their technical assistance. Authors thank Ministère de l'Enseignement Supérieur et de la Recherche. Financial support from Academy of Finland is gratefully acknowledged.

## References

- (1) Yamasaki, A. An Overview of CO<sub>2</sub> Mitigation Options for Global Warming - Emphasizing CO<sub>2</sub> Sequestration Options. *J. Chem. Eng. Jpn.* **2003**, 36 (4), 361.
- (2) Stewart, C.; Hessami, M.-A. A Study of Methods of Carbon Dioxide Capture and Sequestration—the Sustainability of a Photosynthetic Bioreactor Approach. *Energy Convers. Manag.* **2005**, 46 (3), 403.
- (3) Omae, I. Aspects of Carbon Dioxide Utilization. *Catal. Today* **2006**, 115 (1–4), 33.
- (4) McHugh, M.; Krukonic, V. *Supercritical Fluid Extraction: Principles and Practice*; Elsevier, 2013.
- (5) Malik, Q. M.; Islam, M. R. CO<sub>2</sub> Injection in the Weyburn Field of Canada: Optimization of Enhanced Oil Recovery and Greenhouse Gas Storage With Horizontal Wells; Society of Petroleum Engineers, 2000.
- (6) Yu, K. M. K.; Curcic, I.; Gabriel, J.; Tsang, S. C. E. Recent Advances in CO<sub>2</sub> Capture and Utilization. *ChemSusChem* **2008**, 1 (11), 893.
- (7) Olajire, A. A. Valorization of Greenhouse Carbon Dioxide Emissions into Value-Added Products by Catalytic Processes. *J. CO<sub>2</sub> Util.* **2013**, 3-4, 74.
- (8) Demirbaş, A. Biodiesel Fuels from Vegetable Oils via Catalytic and Non-Catalytic Supercritical Alcohol Transesterifications and Other Methods: A Survey. *Energy Convers. Manag.* **2003**, 44 (13), 2093.
- (9) Mohanty, A. K.; Misra, M.; Drzal, L. T. Sustainable Bio-Composites from Renewable Resources: Opportunities and Challenges in the Green Materials World. *J. Polym. Environ.* **2002**, 10 (1-2), 19.
- (10) Rosillo-Calle, F.; Pelkmans, L.; Walter, A. A Global Overview of Vegetable Oils, with Reference to Biodiesel. *Rep. Bioenergy Task* **2009**, 40.

- (11) Sharma, B. K.; Adhvaryu, A.; Liu, Z.; Erhan, S. Z. Chemical Modification of Vegetable Oils for Lubricant Applications. *J. Am. Oil Chem. Soc.* **2006**, *83* (2), 129.
- (12) Figovsky, O.; Shapovalov, L.; Buslov, F. Ultraviolet and Thermostable Non-Isocyanate Polyurethane Coatings. *Surf. Coat. Int. Part B Coat. Trans.* **2005**, *88* (1), 67.
- (13) Leveneur, S.; Zheng, J.; Taouk, B.; Burel, F.; Wärmann, J.; Salmi, T. Interaction of Thermal and Kinetic Parameters for a Liquid–liquid Reaction System: Application to Vegetable Oils Epoxidation by Peroxycarboxylic Acid. *J. Taiwan Inst. Chem. Eng.* **2014**, *45* (4), 1449.
- (14) Tamami, B.; Sohn, S.; Wilkes, G. L. Incorporation of Carbon Dioxide into Soybean Oil and Subsequent Preparation and Studies of Nonisocyanate Polyurethane Networks. *J. Appl. Polym. Sci.* **2004**, *92* (2), 883.
- (15) Javni, I.; Hong, D. P.; Petrović, Z. S. Soy-Based Polyurethanes by Nonisocyanate Route. *J. Appl. Polym. Sci.* **2008**, *108* (6), 3867.
- (16) Li, Z.; Zhao, Y.; Yan, S.; Wang, X.; Kang, M.; Wang, J.; Xiang, H. Catalytic Synthesis of Carbonated Soybean Oil. *Catal. Lett.* **2008**, *123* (3-4), 246.
- (17) Jalilian, M.; Yeganeh, H.; Haghghi, M. N. Preparation and Characterization of Polyurethane Electrical Insulating Coatings Derived from Novel Soybean Oil-Based Polyol. *Polym. Adv. Technol.* **2010**, *21* (2), 118.
- (18) Parzuchowski, P. G.; Jurczyk-Kowalska, M.; Ryszkowska, J.; Rokicki, G. Epoxy Resin Modified with Soybean Oil Containing Cyclic Carbonate Groups. *J. Appl. Polym. Sci.* **2006**, *102* (3), 2904.

- (19) Bähr, M.; Mülhaupt, R. Linseed and Soybean Oil-Based Polyurethanes Prepared via the Non-Isocyanate Route and Catalytic Carbon Dioxide Conversion. *Green Chem.* **2012**, *14* (2), 483.
- (20) Wang, J.; Zhao, Y.; Li, Q.; Yin, N.; Feng, Y.; Kang, M.; Wang, X. Pt Doped  $\text{H}_3\text{PW}_{12}\text{O}_{40}/\text{ZrO}_2$  as a Heterogeneous and Recyclable Catalyst for the Synthesis of Carbonated Soybean Oil. *J. Appl. Polym. Sci.* **2012**, *124* (5), 4298.
- (21) Doll, K. M.; Erhan, S. Z. The Improved Synthesis of Carbonated Soybean Oil Using Supercritical Carbon Dioxide at a Reduced Reaction Time. *Green Chem.* **2005**, *7* (12), 849.
- (22) Mazo, P. C.; Rios, L. A. Improved Synthesis of Carbonated Vegetable Oils Using Microwaves. *Chem. Eng. J.* **2012**, *210*, 333.
- (23) Zhang, L.; Luo, Y.; Hou, Z.; He, Z.; Eli, W. Synthesis of Carbonated Cotton Seed Oil and Its Application as Lubricating Base Oil. *J. Am. Oil Chem. Soc.* **2014**, *91* (1), 143.
- (24) Campanella, A.; Rustoy, E.; Baldessari, A.; Baltanás, M. A. Lubricants from Chemically Modified Vegetable Oils. *Bioresour. Technol.* **2010**, *101* (1), 245.
- (25) Zheng, J. I.; Wärnå, J.; Burel, F.; Salmi, T.; Taouk, B.; Leveneur, S. Kinetic Modeling Strategy for an Exothermic Multiphase Reactor System: Application to Vegetable Oils Epoxidation by Using Prileschajew Method. *AIChE J.* **2015**, doi: 10.1002/aic.15037
- (26) Maerker, G. Determination of Oxirane Content of Derivatives of Fats. *J. Am. Oil Chem. Soc.* **1965**, *42* (4), 329.
- (27) Paquot, C. Standard Methods for the Analysis of Oils, Fats and Derivatives (6th Edition); Pergamon Press Ltd., 1979.

- (28) Burns, J. A.; Verrall, R. E. Thermodynamics of Tetraalkyl- and Bis-Tetraalkylammonium Bromides: II. Heat Capacities of Solid State from 273 to 373 K. *Thermochim. Acta* **1974**, *9* (3), 277.
- (29) Bergman, T. L.; Incropera, F. P.; Lavine, A. S. Fundamentals of Heat and Mass Transfer; John Wiley & Sons, 2011.
- (30) Peng, D.-Y.; Robinson, D. B. A New Two-Constant Equation of State. *Ind. Eng. Chem. Fundam.* **1976**, *15* (1), 59.
- (31) Laugier, F. Les Ultrasons En Procédés Polyphasiques: Transfert Gaz-Liquide, Réaction Liquide-Liquide. 2007.
- (32) Frikha, N.; Schaer, E.; Houzelot, J.-L. Methodology of Multiphase Reaction Kinetics and Hydrodynamics Identification: Application to Catalyzed Nitrobenzene Hydrogenation. *Chem. Eng. J.* **2006**, *124* (1-3), 19.
- (33) Hichri, H.; Accary, A.; Puaux, J. P.; Andrieu, J. Gas-Liquid Mass-Transfer Coefficients in a Slurry Batch Reactor Equipped with a Self-Gas-Inducing Agitator. *Ind. Eng. Chem. Res.* **1992**, *31* (8), 1864.
- (34) Gemo, N.; Biasi, P.; Canu, P.; Salmi, T. O. Mass Transfer and Kinetics of H<sub>2</sub>O<sub>2</sub> Direct Synthesis in a Batch Slurry Reactor. *Chem. Eng. J.* **2012**, *207–208*, 539.